HHS Public Access

Author manuscript

Stroke. Author manuscript; available in PMC 2024 May 01.

Published in final edited form as:

Stroke. 2023 May ; 54(5): 1403–1415. doi:10.1161/STROKEAHA.122.037156.

Deep Imaging to Dissect Microvascular Contributions to White Matter Degeneration in Rodent Models of Dementia

Stefan Stamenkovic, Ph.D.[1,#], **Yuandong Li, Ph.D.**[1,#], **Jack Waters, Ph.D.**[3], **Andy Shih, Ph.D.**[1,2,3,4,*]

[1]Center for Developmental Biology and Regenerative Medicine, Seattle Children's Research Institute, Seattle, WA, USA.

[2]Department of Pediatrics, University of Washington, Seattle, WA, USA.

[3]Allen Institute for Brain Science, Seattle, WA, USA.

[4]Department of Bioengineering, University of Washington, Seattle, WA, USA.

Abstract

The increasing socio-economic burden of Alzheimer's disease and Alzheimer's Disease related dementias (AD/ADRD) has created a pressing need to define targets for therapeutic intervention. Deficits in cerebral blood flow and neurovascular function have emerged as early contributors to disease progression. However, the etiology, progression, and consequence of small vessel diseases in AD/ADRD remains poorly understood, making therapeutic targets difficult to pinpoint. Animal models that recapitulate features of AD/ADRD may provide mechanistic insight because microvascular pathology can be studied as it develops in vivo. Recent advances in in vivo optical and ultrasound-based imaging of the rodent brain facilitate this goal by providing access to deeper brain structures, including white matter and hippocampus, which are more vulnerable to injury during cerebrovascular disease. Here, we highlight these novel imaging approaches and discuss their potential for improving our understanding of vascular contributions to AD/ADRD.

INTRODUCTION

Progressive cognitive decline during AD/ADRD is one of the leading health problems of our time and effective clinical treatments have remained elusive. AD/ADRD includes dementias involving cerebrovascular disease, referred to as vascular contributions to cognitive impairment and dementia (VCID). Reduction in cerebral blood flow is a contributing factor to AD/ADRD progression, and has been widely reported in human patients and animal models of dementia.[1] In fact, large cohort clinical studies indicate that cerebral blood flow reduction and neurovascular dysregulation occurs early in the cascade of pathological events leading to AD/ADRD, preceding amyloid beta deposition, cerebral hypometabolism, and cognitive decline.[2–4] This suggests that neurovascular dysfunction is

[*]**Correspondence:** Andy Y. Shih, Center for Developmental Biology and Regenerative Medicine, Seattle Children's Research Institute, 1900 9th Ave. M/S JMB-5, Seattle, WA 98101, Office: 206-884-1314, Fax: 206-884-1407, Andy.Shih@SeattleChildrens.org.
[#]These authors contributed equally

Disclosures. None

a relevant treatment target that should be engaged early in disease progression. However, these data also emphasize our lack of knowledge on how neurovascular dysfunction is initiated in AD/ADRD. For example, what are the earliest molecular and cellular changes in the vascular wall that lead to degradation of the brain microvasculature, and what events trigger these changes? What locations within the vascular tree (arteriole-capillary-venous) are affected first, and what effect do these changes have on overall cerebral blood flow, brain metabolism and neuronal function? How do vascular beds of the more vulnerable tissues such as white matter and the hippocampus differ from more resilient tissues? Which of the many vascular abnormalities seen in AD/ADRD are truly disease-driving, and are they reversible? Answering these questions will improve our ability to find rational strategies for mitigation of neurovascular impairment in AD/ADRD.

Although rodent models cannot fully capture the diverse and complex disease processes of human AD/ADRD[5, 6], studies suggest that many models recapitulate aspects of small vessel disease and blood flow impairment seen in the human condition (reviewed by Szu et al.[7], Bracko et al.[1], and Shih et al.[8]).[1, 7] A range of microvascular abnormalities can be studied in rodents, including cerebral amyloid angiopathy (CAA), abnormal vessel tone/reactivity, increased vascular tortuosity, reduced capillary density, and blood-brain barrier permeability. The neuropathological outcomes of these changes, including hemorrhage, small cortical/subcortical infarcts, microbleeds/microinfarcts, white matter degeneration/myelin pallor, and neuroinflammation are also seen in many models. This provides an opportunity to use advanced high-resolution in vivo imaging to study how small vessel pathologies originate and contribute to dysfunction of neurovascular cell types and surrounding neurons and myelin.

The wealth of clinical imaging studies using MRI point to the vulnerable cerebral white matter as a region of emphasis for preclinical imaging studies. Degeneration of periventricular white matter (apparent as white matter hyperintensities on MRI) is associated with worsened cognitive outcomes in AD/ADRD.[9, 10] Interestingly, neuroimaging data also suggest that degeneration of superficial white matter tracts (or U fibers) is also an early event in the progression of AD/ADRD and related to cognitive decline.[11–13] In rodent studies, the corpus callosum (CC) and the external capsule (EC) are the largest and most commonly study white matter regions and are analogous to human U fibers. In both rodents and humans, these fibers reside directly beneath the cortex and support cortico-cortical communication. Preclinical studies have shown specific deterioration of the CC/EC with aging and when challenged by disease processes, including tissue atrophy, increased gliosis and inflammation, and loss of myelin.[14–18] However, the etiology of tissue deterioration in white matter, even in rodent models of AD/ADRD, remains poorly understood because most prior studies have been cross-sectional in time. Thus, longitudinal imaging of live mouse models provides an opportunity to better understand the vascular networks that perfuse superficial white matter, and the potential bases of their deterioration in AD/ADRD.

MRI has been used extensively to investigate changes in vascular structure and function[19], microhemorrhages[20], development of Aβ plaques[21], and white matter pathology[22] in rodent models of AD/ADRD. Similarly, PET has been used to investigate development of CAA[23] and Aβ plaques[24], amyloid load[25], neuroinflammation and glial reactivity[26], as well as

brain metabolism and function[27]. However, these modalities lack the ability to resolve microvessel perfusion and cellular changes in endothelial cells, smooth muscle cells, pericytes, astrocytes, and microglia. Traditional approaches to measure vascular structure and cerebral blood flow, such as histology and cerebral blood flow autoradiography capture only a moment-in-time during the evolution of the disease. The hydrogen clearance method, a technique used for measurements of blood flow using an inserted probe, also lacks spatial resolution and can lead to tissue damage.

This review will focus on emergent high-resolution imaging technologies that are poised to transform our understanding of how neurovascular pathology contributes to AD/ADRD (Table 1). These technologies would allow preclinical researchers to: (1) image deeper into the brain to observe white matter in vivo with minimal perturbation of the cortex; (2) image longitudinally starting before the onset of pathological changes; (3) use animal models that reveal changes in different neurovascular cell types; and (4) study mice in the awake or lightly sedated states to avoid confounding effects of anesthesia on neurovascular physiology.[28, 29]

TWO-PHOTON MICROSCOPY

The development of two-photon fluorescence microscopy (2PM) by Denk and colleagues in 1990 revolutionized in vivo optical imaging.[30] Two-photon excitation requires the near-simultaneous arrival of two photons at the fluorophore to be observed in vivo. The probability of two-photon excitation is low, except at the focus of the microscope objective where photon density is high. Fluorophores above and below the focal plane are not sufficiently excited, and this produces optical tissue sectioning necessary to reconstruct complex 3D structures at sub-micrometer to micrometer resolution. Two-photon imaging also uses longer wavelengths of light that penetrate further into tissues and reduces likelihood of photo-damage.

The parallel development of approaches to fluorescently label neurons and astrocytes allowed detailed study of neuroanatomy[31], neural activity[32], and neuro-glio-vascular interactions[33]. Intravenous injection of high molecular weight fluorescent dyes enabled visualization of vascular architecture and blood cell movement, facilitating studies of the microvasculature.[34, 35] Development of transgenic lines that labeled neurovascular cell types opened the door to in vivo studies of the neurovascular unit.[36, 37] Two-photon microscopy is now a widely used technique for studying many aspects of the brain vasculature, including but not limited to neurovascular coupling[38–43], development of the neurovasculature[44–46], immune cell-neurovascular interactions[47, 48], brain tissue oxygenation[49–52], blood-brain barrier function[53, 54], and perivascular clearance.[55, 56]

DEEP TWO-PHOTON MICROSCOPY

Despite its advantages, the penetration depth of 2PM is still limited for studying deeper brain structures. In mice, the white matter tract of the corpus callosum is ~0.8 to 1 mm below the cortical surface, and the hippocampus is 1 to 2 mm deep. Conventional 2PM can generally reach ~0.5 mm in depth, which corresponds to the upper half of the cortex.

The wavelengths of light used during conventional 2PM (800–1000 nm) reach a limit in depth penetration because they are absorbed superficially by tissue. This limitation led to the development of “deep 2PM”, which uses lasers that emit longer excitation wavelengths, ranging from 1100–1300 nm, to access an optical window with lower light absorption to excite fluorophores with red to far-red shifted fluorescence.[57, 58]

The depth penetration advantage of deep 2PM was first demonstrated by Kobat et al. They used 1280 nm excitation and Alexa 680-dextran to image mouse cortical vasculature between 1 to 1.6 mm below the cortical surface, which accessed corpus callosum and hippocampus.[57 59] They further showed that functional measurements of blood flow in individual capillaries could be achieved at ~0.9 mm depth. Separately, Miller et al. demonstrated blood flow measurements down to 1.2 mm in depth, and structural imaging of microvasculature at ~1.5 mm.[58] This was achieved by imaging Texas Red labeled blood plasma using high energy pulses and long excitation wavelengths (1215 nm). Further, they established the feasibility of imaging TdTomato-labeled neurons in the corpus callosum at ~1 mm in depth, suggesting that 2PM can be useful for imaging neurovascular cell types in white matter of transgenic mice.

Li et al. used deep 2PM to measure blood flow in capillaries throughout the cortex and into the callosal white matter (Fig. 1A,B) in healthy mice during normocapnia and mild hypercapnia, and under global cerebral hypoperfusion induced by bilateral carotid artery stenosis.[60] They showed that capillary blood flow under basal conditions is significantly higher in the callosal white matter compared to the adjacent cortical gray matter and exhibits a much smaller fractional increase in response to mild hypercapnia. However, during global cerebral hypoperfusion, white matter capillary blood flow is significantly reduced, while capillary flow is relatively preserved in the cortical gray matter (Fig. 1C). This is consistent with callosal white matter being a perfusion watershed that is more susceptible during global hypoperfusion. It also suggests that autoregulatory dilation of cerebral arteries and arterioles is insufficient to maintain perfusion in white matter.

THREE-PHOTON MICROSCOPY

While the imaging depth achieved by deep 2PM is greater than that of conventional 2PM, it is still difficult in practice to reach the corpus callosum and beyond. A reduction in signal-to-background ratio occurs in deeper tissues because a smaller percentage of the incident photons reach the focus, and a higher percentage of photons drive out-of-focus excitation.[61, 62] This makes it increasingly more difficult to distinguish fluorescent microstructures from background signal. Another limitation of deep 2PM is that it relies on red fluorophores, while many established reporters of cellular morphology and activity are green. Three-photon microscopy (3PM) overcomes these limitations by requiring three photons to simultaneously interact with a fluorophore at the focal plane to generate emission photons. This reduction in the probability of photon interaction further reduces out-of-focus fluorescence and improves the signal-to-background ratio at greater depths in the brain tissue.[63, 64]

3PM uses a distinct pulsed laser source that provides higher peak power for excitation but with lower repetition rate to reduce average power and likelihood of photodamage. As with deep 2PM, excitation wavelengths for 3PM are centered around windows of reduced light absorption by tissue (1300 nm and 1700 nm).[63] 3PM also enables deep imaging of well characterized fluorescent dyes and proteins in the green emission range (Fig. 1D–F; green is genetically-encoded calcium indicator, GCaMP6).[65–68] Further, an intrinsic third harmonic generation (THG) signal from myelin can be used to define cerebral white matter (Fig. 1D,E; magenta). The transition from cortical gray matter to sub-cortical white matter could be defined during in vivo 3PM by observing myelinated tracts as they shift from a vertical orientation in cortical layer 6 to horizontal orientation in the EC (Fig. 1E). Interestingly, blood vessels also generate a THG signal and can be discerned in the less myelinated gray matter (Fig. 1D,E).

The feasibility of imaging subcortical structures using 3PM was first shown by Horton et al.[63] They used 1700 nm excitation to image Texas Red-labeled vasculature and red fluorescent protein (RFP)-labeled neurons in the CA1 region of the hippocampus, at 1.1 to 1.3 mm below the cortical surface. Ouzounov et al. then demonstrated functional imaging of Ca^{2+} activity in GCaMP6 labeled CA1 hippocampal neurons using 1300 nm excitation (Fig. 1F).[68] Vascular structure and calcium activity in GCaMP6-labeled or Oregon Green Bapta-labeled neurons of the mouse visual cortex were imaged up to 1 mm in depth, reaching deep cortical layers and white matter[65, 69] More recently, Thornton et al.[67] imaged transgenic mice that expressed tdTomato in oligodendrocyte lineage cells and eGFP in mature oligodendrocytes, and demonstrated the visualization of these myelin producing cells at depths up to 1.1 mm. Similarly, Hontani et al.[66] used 3PM at 1340 nm for multi-color fluorescence imaging of green fluorescent GCaMP6s-labeled neurons, red fluorescent Texas Red–labeled blood vessels, and THG signal from myelinated axons. This enabled concurrent functional imaging of neuronal activity and vascular structure in the subcortical white matter tracts up to ~1 mm of cortical depth. Further, recent work also demonstrated imaging of sulforhodamine-labeled astrocytes up to 1.3 mm into the mouse brain using 1700 nm excitation.[70] Collectively, these studies highlight the potential for multi-color, multi-cellular imaging in deep cortex and white matter using 3PM.

Koizumi et al., applied 3PM to a mouse model relevant to AD/ADRD.[15] They imaged microvasculature in the corpus callosum of transgenic mice carrying the human Apoe4 allele, a key genetic risk factor for sporadic AD and VCID. The Apoe4 allele is associated with worsened pericyte survival[54], blood-brain barrier deficiency, and cognitive impairment.[71] Koizumi et al. showed a reduction of blood flow velocity at baseline in white matter capillaries of Apoe4 mice, but not control Apoe3 mice. In response to a 4-week challenge to cerebral hypoperfusion by bilateral common carotid artery stenosis, Apoe4 mice showed a greater reduction in capillary flow in white matter. Furthermore, this reduction in blood flow was linked to local hypoxia and white matter damage, indicating that capillary flow deficits may also contribute to increased risk in Apoe4 carriers.

OPTICAL COHERENCE TOMOGRAPHY

Optical coherence tomography (OCT) is a 3D optical imaging technique to visualize tissue microstructure and vasculature in the living brain.[72] The principle of OCT is analogous to ultrasound imaging, measuring echo time delay of backscattered light. The backscattered light is measured with an interferometric set-up that analyzes the combined light waves from the sample and a reference mirror to reconstruct the depth profile of the imaged sample. A scanning OCT beam allows for acquisition of cross-sectional images in the axial dimension, and this beam can be rapidly swept across the brain surface to achieve 3D imaging at high frequency. The imaging contrast is generated from the intrinsic scattering properties of tissue components, displaying different aspects of tissue structure and vasculature without exogenous contrast agents.[73] For example, OCT angiography (OCTA) can map cerebral blood vessels based on the dynamic scattering of moving blood cell.[74, 75] Compared with multiphoton imaging, OCTA has lower spatial resolution (~10–15 μm) but much faster image acquisition speed and can assess capillary architecture within a cubic millimeter of brain tissue in vivo within a matter of seconds. As with deep 2PM and 3PM, 1300 nm and 1700 nm are two spectral windows for OCT imaging of deep brain tissue with the least light absorption.

Prior studies showed that 1300 nm OCTA can be used to resolve microvascular structure in vivo from the pial surface to the corpus callosum in the mouse barrel cortex through a cranial window (Fig. 2A).[76] A dynamic focusing approach was used by integrating an electrically tunable lens in the scanning optics to overcome the depth of focus limitation and enhance deep vascular imaging. The large branches of principal cortical venules are prominent at the interface between cortical layer 6 and underlying white matter and can be seen alongside smaller capillary sized vessels (Fig. 2A). These venules are thought to be drainage outputs for blood from the white matter.[77] Using 1700 nm OCTA, studies have probed larger blood vessels in the mouse corpus callosum and hippocampus, though the resolution of capillary-sized vessels was diminished.[78] In addition to vascular structure, axial blood flow velocity (velocity in the flow direction that is parallel to the scanning beam) can be also measured (Fig. 2B).[79–81] Proof-of-principle measurements of blood flow have been taken from larger branches of principal cortical venules in the corpus callosum.[76]

OCTA has been used to study cerebrovascular diseases. For example, imaging of blood flow in pial and penetrating arterioles after middle cerebral artery occlusion have revealed how collateral arterioles re-distribute blood flow in penetrating arterioles throughout the cortex.[82–84] OCTA has also been used to study age-related differences in cerebrovascular anatomy and hemodynamics, which has revealed an increase in arterial tortuosity and decrease in capillary density and cerebral blood flow in aged animals.[85] The technique has also advanced considerably for high throughput, broad-scale measurements of capillary flow in vivo at least up to 0.5 mm in depth (Fig. 2C).[86–88] Capillary transit time heterogeneity (CTTH) can now be studied in detail in mice.[89] At resting state, the speed of RBCs among capillary segments are extremely heterogeneous.[35] During neural activation, flux among capillary segments homogenize (decreased CTTH) to facilitate a more efficient oxygen distribution and extraction.[90] Increased CTTH has been implicated in AD/ADRD[91], and

animal models may help to establish the underpinnings of this change in brain capillary perfusion.

OPTICAL COHERENCE MICROSCOPY

Optical coherence microscopy (OCM) was developed to combine the principle of OCT with confocal microscopy, making it possible to resolve neuronal cell bodies and myelination.[92] The imaging contrast of OCM also arises from the intrinsic light scattering property of the tissue against the background. For instance, neuron cell bodies manifest as low scattering regions against a highly scattering background of neurites, and myelinated axons manifest as highly backscattering signals.[92] Based on these properties, minimum and maximum intensity projections can be produced to visualize neuronal cell bodies and myelination, respectively (Fig. 2D,E).[93] OCM imaging could reach the mouse corpus callosum where laterally projecting myelinated axon tracts were visible. In the 5xFAD mouse model of AD where amyloid burden develops earliest in the deep cortical layers, a recent study revealed co-occurring demyelination primarily in deep cortical layers.[93]

PHOTOACOUSTIC IMAGING

Photoacoustic tomography (PAT) achieves deep imaging by combining light and ultrasound into a single technology. Short pulses of light are used to induce local thermoelastic expansions in tissues, creating low scattering ultrasound waves that pass easily through soft tissues.[94] These emitted waves are detected using ultrasonic transducers spatially arranged around the animal's head and the 3D image is formed by triangulating the location from which the waves originate. Oxyhemoglobin strongly absorbs wavelengths of light used during PAT (i.e., 532 nm), and signal generation from the blood enables in vivo imaging of the microvasculature.

PAT has been used to image vascular structure and blood oxygenation in small rodents at various spatial scales, often through the intact skull to preserve the intracranial environment.[95, 96] Within the spatial ranges relevant to imaging of cerebral microvessels in vivo, lateral resolutions of 10 to 100 μm can be achieved at depths at least 1–3 mm deep. Small vessels throughout the white matter and subcortical tissues can be visualized (Fig. 3A).[97] A particularly strong signal generator is the inferior sagittal sinus and its branches suggesting it is possible to longitudinally track mid- to large-sized veins/sinuses that collect blood from deep medial surfaces of the brain hemispheres.[96] Further, the differing absorption properties of deoxy- and oxyhemoglobin and the ability to perform fast successive scanning allows total blood hemoglobin, oxygen saturation of hemoglobin, and blood flow velocity to be measured concurrently with vascular structure (Fig. 3B).[98, 99] From these parameters, the oxygen extraction fraction (OEF) and cerebral metabolic rate of oxygen (CMRO2) can be estimated for investigations of neurovascular coupling, although only within cortex at this stage.[100] As a proof-of-principle for dementia-related studies, PAT is sensitive to decreases in cortical cerebral blood flow and CMRO2 induced by amyloid plaque accumulation and CAA in the arcAβ mouse model of AD[101] and in response to brief periods of hypoxic challenge.[99]

Higher resolutions can be achieved with further adaptations, such as focusing of the excitation light through microscope objectives and use of advanced detectors, albeit with a tradeoff in imaging depth.[96] Optical-resolution photoacoustic microscopy (OR-PAM) involves imaging through a cranial window and focusing of the excitation light through an objective, which increases sensitivity to contrast and achieves cellular resolution, with tradeoffs in in depth penetration and acquisition speed.[102] Hu et al. showed that OR-PAM could be used to image amyloid plaques in APP/PS1 mice in vivo.[103] The mice were injected with Congo red through the cisterna magna and imaging with both OR-PAM and 2PM revealed correlation in plaque distribution between modalities.[103]

FUNCTIONAL ULTRASOUND IMAGING

Functional ultrasound (fUS) imaging is a noteworthy emergent technique for imaging cerebral hemodynamics in animal models.[104] It has depth advantages over modalities requiring optical excitation, as it uses ultrasound waves to both stimulate and detect, which increases signal transmission for whole brain imaging of cerebral hemodynamics up to 1 cm in depth. It also provides a lateral resolution of ~100 μm across a 300 μm slice of tissue in the coronal plane, with high temporal resolution (10 Hz)(Fig. 3C).[105] While fUS lacks resolution to observe the structure of individual penetrating vessels, and can detect relative change in blood flow within perfusion domains of individual cortical and subcortical arterioles and venules (Fig. 3D).[106] Functional ultrasound measurements are often used as a proxy for neural activity in studies of functional hyperemia and resting state connectivity in awake mice.[107]

An adaptation of fUS called ultrasound localization microscopy (ULM) substantially increases the imaging resolution of fUS, but with longer integration time (Fig. 3E,F).[108] This involves injection of inert gas microbubbles and tracking of individual microbubbles within the blood stream to obtain quantitative and localized maps of blood flow velocity at the spatial scale of ~10 μm in 100 μm thick coronal slices. Recently, ULM was applied to the imaging of adult and aged mouse brain in vivo, revealing that the approach can detect age-related decreases in cerebral blood flow and increased tortuosity of penetrating vessels.[109]

CHOOSING AN APPROACH

The technologies reviewed here enable studies of vascular function in the white matter and deeper structures of live rodents. They span a range of spatiotemporal scales, and each have advantages and disadvantages (Table 2). This requires investigators to match the technique to the biological question. Deep 2PM and 3PM would be ideal for studying vascular function at the level of single arterioles, capillaries, and venules. They provide the highest resolution and versatility for imaging cell types of the neurovascular unit and surrounding neural tissue but are low throughput from broader measurements of blood flow. OCTA is preferred for study of microvascular network dynamics with its ability to sample flow across many vessels at once with high spatiotemporal resolution. However, it is not well suited for examining small changes in vascular diameter and does not permit the concurrent study of neurovascular cell types. OCM provides cellular-level, label-free imaging of myelinated

tissues to query disease-related changes to the white matter. Photoacoustic imaging provides a further tradeoff in spatial resolution for imaging depth, being able to reach several millimeters into the brain through an intact or thinned skull. The oxygenation state of blood can be measured without exogenous agents, which is a unique benefit over other techniques. However, capillary-level changes may not be resolvable at depth. Finally, fUS is preferred for deep imaging of relative change in cerebral blood flow with a further tradeoff in imaging resolution, though ULM greatly increases resolution with microbubble tracking. A mix of multiple imaging modalities within a lab would help researchers strike the right balance between spatial resolution, imaging depth, and ability to measure the relevant biological processes for their research questions.[106]

PROSPECTIVE STUDIES AND OPPORTUNITIES

When applied to mouse models that recapitulate aspects of human AD/ADRD, these recent advances in deep imaging can add significant insight into how early microvascular dysfunction contributes to degeneration of white matter and other deep brain structures. Numerous aspects of neurovascular physiology and pathophysiology can be addressed, and our discussion of prospective studies/opportunities below is by no means exhaustive. Rather, they are example topics that would build foundational knowledge of how vascular structure and perfusion differs between deep brain tissues and the well-studied cerebral cortex.

Angioarchitecture and perfusion of gray matter versus superficial white matter.

More data is needed to understand the basic structural and functional properties of the vascular networks that perfuse the cerebral white matter. Deep 2PM and 3PM can be used to gather information on 3D vascular structure, pathways for arteriole-capillary-venous perfusion, and vascular physiology (functional reactivity, vasomotor oscillations) in the CC/EC and deeper subcortical tissues. Given the heterogeneity of perfusion dynamics in the variety of small vessel types, these data collected initially from normal adult and aged mice would be an essential baseline to understand normal age-related changes in vascular function. Upon these data, it is then logical to ask how small vessel disease processes can trigger vascular abnormalities in models of AD/ADRD. Venous drainage systems would be equally as important to study as arterioles and capillaries, since all blood entering a tissue must also exit, and there is evidence for small vessel disease of venules in white matter, i.e., venous collagenosis and increased tortuosity, with physiological impact still poorly understood.[110, 111] Complementing deep 2PM and 3PM, OCTA, photoacoustic imaging, and fUS can then provide broader scale imaging to determine overall changes in cerebral perfusion in penetrating arterioles and venules that supply and drain the white matter.

Differences in capillary flow dynamics in gray versus white matter.

The capillary network is optimized to ensure that all capillaries have some degree of perfusion at rest, yet provides room for augmented flow (homogenization) during brain activity.[90] However, aging is associated with increased capillary tortuosity, formation of non-patent string capillaries, alterations in capillary diameter as well as reduction of capillary density, and these abnormalities are exacerbated with AD/ADRD.[17, 112] Further, capillary flow stalling by adherent leukocytes is increased in AD mouse models and

contributes to cerebral hypoperfusion.[48, 113] The accumulation of these defects can impair the distribution of blood in the capillary network at rest and raise the threshold to achieve flux homogenization. Indeed, recent studies have used dynamic susceptibility contrast MRI to infer dysfunction in the transit of blood through brain capillaries in AD.[114] It is possible that capillary beds in white matter experience earlier and more severe deviations from normal capillary flow heterogeneity, compared to upper layers of cortex. Longitudinal deep multiphoton imaging and OCTA will help to address this open question. OCTA capillary velocimetry has captured the process of capillary flow homogenization during functional hyperemia, and it was shown that capillary hemodynamics in the aged mouse brain exhibits increased capillary velocity heterogeneity compared to younger mice.[85] However, these measurements were restricted to the upper layers of cortex, and deeper imaging is needed to determine how capillary dysfunction unfolds in white matter. Further, capillary flow dynamics have been measured in some AD/ADRD models but have similarly been restricted to the upper layers of cortex.[48, 113, 115, 116]

Differences in pericyte function and viability in cortex versus deep tissues.

Pericytes are mural cells of the capillary network that play critical roles in maintenance of blood-brain barrier integrity.[117–120] Pericytes are highly sensitive to cerebrovascular pathology, and studies have shown significant loss in pericyte density and coverage in both normal aging[121] and AD/ADRD[122–125] However, whether pericyte loss is a driver of capillary deterioration or a consequence remains unclear. Recent studies have used strategies to induce pericyte loss in the adult brain while examining capillary flow dynamics. They suggest that pericyte loss is sufficient to cause abnormal redistribution of blood flow in capillary networks, stalling of blood cells, and vascular regression.[126, 127] No information is available on the effect of pericyte loss on capillary perfusion in the cerebral white matter and the hippocampus. Further, questions remain on what causes pericyte loss in AD/ADRD. Recent studies have suggested that amyloid beta induces expression of endothelin-1 that leads to aberrant contraction of pericytes.[128] It is presumed that this over-activation in the presence of amyloid beta could also initiate pericyte death, and this can be ascertained by deep imaging in AD models with fluorescently labeled pericytes. Further, the Iowa amyloid beta mutation tends to cause capillary-level CAA (CAA Type 1), while the Dutch mutation tends to accumulate in larger arterioles (CAA type 2), suggesting that different amyloid beta forms can trigger different cerebrovascular outcomes, warranting investigation across CAA models.[129]

A recent study revealed that differences in hippocampal vasculature that may underlie increased vulnerability to pathology, including reduced capillary diameter, density and dilatory responses to neural activity, compared to the visual cortex.[130] Pericyte density was also reduced in hippocampus, as was the distribution of pericyte subtypes with more contractile phenotypes. This pioneering in vivo imaging study was conducted with conventional 2PM and required removal of the cortex. Deep 2PM and 3PM imaging could provide more noninvasive deep tissue access to build upon these observations.

What vascular changes precede neurodegeneration?

The structure and function of neurons should be considered alongside vascular changes in longitudinal imaging studies to better understand which aspects of neurovascular dysfunction precede and are therefore potential drivers of neurodegeneration. During aging in rodents, neuronal numbers remain largely unchanged, but there is a gradual loss of myelin and oligodendrocytes.[131] During age-related white matter loss cases in humans and non-human primates, there is similarly a loss of myelinated nerve fibers.[132, 133] These changes affect conduction efficiency in neuronal circuits and are associated with reduction of cognitive function. [134] Myelin loss is also prominent in AD/ADRD, and can precede Aβ and tau pathologies.[135] When and what type of vascular insufficiencies occur in white matter in relation to this myelin loss is important to clarify. In this context, both 3PM and OCM offer the ability to measure the integrity of myelinated axons in deep cortex and white matter while tracking the evolution of neurovascular pathology in AD/ADRD models. As discussed above, OCM has revealed changes in myelination in the deep cortex of 5xFAD mice with AD amyloid pathology[93], and 3PM can be useful for dual imaging of vasculature and the oligodendrocyte populations that construct the myelin sheaths.[67]

Conclusions.

Emergent deep imaging technologies are being applied to AD/ADRD-relevant questions, but current applications have only scratched the surface in their potential to reveal mechanistic insight. Deeper imaging is needed to understand the microvascular bases of white matter degeneration, and to ensure that studies are applied to clinically relevant brain structures vulnerable in AD/ADRD.

Funding.

Our work is supported by grants to A. Shih from the NIH/NINDS (NS097775) and NIH/NIA (AG063031, AG062738, R21AG069375, RF1AG077731).

Abbreviations:

2PM	Two-photon fluorescence microscopy
3PM	Three-photon microscopy
AD/ADRD	Alzheimer’s disease and Alzheimer’s Disease-related dementias
CAA	Cerebral amyloid angiopathy
CC	Corpus callosum
CTTH	Capillary transit time heterogeneity
EC	External capsule
fUS	Functional ultrasound
MRI	Magnetic resonance imaging
OCM	Optical coherence microscopy

OCT	Optical coherence tomography
OCTA	Optical coherence tomography angiography
PAT	Photoacoustic tomography
PET	Positron emission tomography
THG	Third harmonic generation
ULM	Ultrasound localization microscopy
VCID	Vascular contributions to cognitive impairment and dementia

REFERENCES

1. Bracko O, Cruz Hernández JC, Park L, Nishimura N, Schaffer CB. Causes and consequences of baseline cerebral blood flow reductions in Alzheimer's disease. Journal of cerebral blood flow and metabolism. 2021;41:1501–1516 [PubMed: 33444096]
2. Leijenaar JF, van Maurik IS, Kuijer JPA, van der Flier WM, Scheltens P, Barkhof F, Prins ND. Lower cerebral blood flow in subjects with Alzheimer's dementia, mild cognitive impairment, and subjective cognitive decline using two-dimensional phase-contrast magnetic resonance imaging. Alzheimer's & dementia. 2017;9:76–83
3. Iturria-Medina Y, Sotero RC, Toussaint PJ, Mateos-Pérez JM, Evans AC, Alzheimer's Disease Neuroimaging Initiative. Early role of vascular dysregulation on late-onset Alzheimer's disease based on multifactorial data-driven analysis. Nature Communications. 2016;7:11934
4. Binnewijzend MA, Benedictus MR, Kuijer JP, van der Flier WM, Teunissen CE, Prins ND, Wattjes MP, van Berckel BN, Scheltens P, Barkhof F. Cerebral perfusion in the predementia stages of Alzheimer's disease. European Radiology. 2016;26:506–514 [PubMed: 26040647]
5. Wardlaw JM, Smith C, Dichgans M. Small vessel disease: Mechanisms and clinical implications. Lancet Neurology. 2019;18:684–696 [PubMed: 31097385]
6. Iadecola C The pathobiology of vascular dementia. Neuron. 2013;80:844–866 [PubMed: 24267647]
7. Szu JI, Obenaus A. Cerebrovascular phenotypes in mouse models of Alzheimer's disease. Journal of cerebral blood flow and metabolism. 2021;41:1821–1841 [PubMed: 33557692]
8. Shih AY, Hyacinth HI, Hartmann DA, van Veluw SJ. Rodent models of cerebral microinfarct and microhemorrhage. Stroke. 2018;49:803–810 [PubMed: 29459393]
9. Garnier-Crussard A, Bougacha S, Wirth M, Dautricourt S, Sherif S, Landeau B, Gonneaud J, De Flores R, de la Sayette V, Vivien D, et al. White matter hyperintensity topography in Alzheimer's disease and links to cognition. Alzheimer's & dementia. 2021;18:422–433
10. Wardlaw JM, Smith EE, Biessels GJ, Cordonnier C, Fazekas F, Frayne R, Lindley RI, O'Brien JT, Barkhof F, Benavente OR, et al. Neuroimaging standards for research into small vessel disease and its contribution to ageing and neurodegeneration. Lancet Neurology. 2013;12:822–838 [PubMed: 23867200]
11. Fornari E, Maeder P, Meuli R, Ghika J, Knyazeva MG. Demyelination of superficial white matter in early Alzheimer's disease: A magnetization transfer imaging study. Neurobiology of Aging. 2012;33:428.e427–419
12. Reginold W, Luedke AC, Itorralba J, Fernandez-Ruiz J, Islam O, Garcia A. Altered superficial white matter on tractography mri in Alzheimer's disease. Dementia and geriatric cognitive disorders extra. 2016;6:233–241 [PubMed: 27489557]
13. Phillips OR, Joshi SH, Piras F, Orfei MD, Iorio M, Narr KL, Shattuck DW, Caltagirone C, Spalletta G, Di Paola M. The superficial white matter in Alzheimer's disease. Human brain mapping. 2016;37:1321–1334 [PubMed: 26801955]
14. Shibata M, Ohtani R, Ihara M, Tomimoto H. White matter lesions and glial activation in a novel mouse model of chronic cerebral hypoperfusion. Stroke.35:2598–2603

15. Koizumi K, Hattori Y, Ahn SJ, Buendia I, Ciacciarelli A, Uekawa K, Wang G, Hiller A, Zhao L, Voss HU, et al. Apoε4 disrupts neurovascular regulation and undermines white matter integrity and cognitive function. Nature Communications. 2018;9:3816
16. Reeson P, Choi K, Brown CE. VEGF signaling regulates the fate of obstructed capillaries in mouse cortex. Elife. 2018;7
17. Schager B, Brown CE. Susceptibility to capillary plugging can predict brain region specific vessel loss with aging. Journal of Cerebral Blood Flow & Metabolism. 2020;40:2475–2490 [PubMed: 31903837]
18. Liu H, Yang Y, Xia Y, Zhu W, Leak RK, Wei Z, Wang J, Hu X. Aging of cerebral white matter. Ageing Research Reviews. 2017;34:64–76 [PubMed: 27865980]
19. Kara F, Dongen ES, Schliebs R, Buchem MA, Groot HJ, Alia A. Monitoring blood flow alterations in the Tg2576 mouse model of Alzheimer's disease by in vivo magnetic resonance angiography at 17.6 t. Neuroimage. 2012;60:958–966 [PubMed: 22227054]
20. Poduslo JF, Hultman KL, Curran GL, Preboske GM, Chamberlain R, Marjańska M, Garwood M, Jack CRJ, Wengenack TM. Targeting vascular amyloid in arterioles of Alzheimer disease transgenic mice with amyloid β protein antibody-coated nanoparticles. Journal of Neuropathology and Experimental Neurology. 2011;70:653–661 [PubMed: 21760540]
21. Braakman N, Matysik J, van Duinen SG, Verbeek F, Schliebs R, de Groot HJ, Alia A. Longitudinal assessment of Alzheimer's beta-amyloid plaque development in transgenic mice monitored by in vivo magnetic resonance microimaging. Journal of Magnetic Resonance Imaging. 2006;24:530–536 [PubMed: 16892201]
22. Song SK, Kim JH, Lin SJ, Brendza RP, Holtzman DM. Diffusion tensor imaging detects age-dependent white matter changes in a transgenic mouse model with amyloid deposition. Neurobiology of Disease. 2004;15:640–647 [PubMed: 15056472]
23. Han BH, Zhou ML, Vellimana AK, Milner E, Kim DH, Greenberg JK, Chu W, Mach RH, Zipfel GJ. Resorufin analogs preferentially bind cerebrovascular amyloid: Potential use as imaging ligands for cerebral amyloid angiopathy. Molecular Neurodegeneration. 2011;6 [PubMed: 21244648]
24. Snellman A, López-Picón FR, Rokka J, Salmona M, Forloni G, Scheinin M, Solin O, Rinne JO, Haaparanta-Solin M. Longitudinal amyloid imaging in mouse brain with 11c-pib: Comparison of APP23, Tg2576, and APPswe-PS1dE9 mouse models of Alzheimer disease. Journal of nuclear medicine. 2013;54:1434–1441 [PubMed: 23833271]
25. Cohen RM, Rezai-Zadeh K, Weitz TM, Rentsendorj A, Gate D, Spivak I, Bholat Y, Vasilevko V, Glabe CG, Breunig JJ, et al. A transgenic Alzheimer rat with plaques, tau pathology, behavioral impairment, oligomeric aβ, and frank neuronal loss. Journal of neuroscience. 2013;33:6245–6256 [PubMed: 23575824]
26. Maeda J, Zhang MR, Okauchi T, Ji B, Ono M, Hattori S, Kumata K, Iwata N, Saido TC, Trojanowski JQ, et al. In vivo positron emission tomographic imaging of glial responses to amyloid-beta and tau pathologies in mouse models of Alzheimer's disease and related disorders. Journal of neuroscience. 2011;31:4720–4630 [PubMed: 21430171]
27. Poisnel G, Hérard AS, El Tannir El Tayara N, Bourrin E, Volk A, Kober F, Delatour B, Delzescaux T, Debeir T, Rooney T, et al. Increased regional cerebral glucose uptake in an APP/PS1 model of alzheimer's disease. Neurobiology of Aging. 2012;33:1995–2005 [PubMed: 22079157]
28. Gao YR, Ma Y, Zhang Q, Winder AT, Liang Z, Antinori L, Drew PJ, Zhang N. Time to wake up: Studying neurovascular coupling and brain-wide circuit function in the un-anesthetized animal. Neuroimage. 2017;153:382–398 [PubMed: 27908788]
29. Grutzendler J, Nedergaard M. Cellular control of brain capillary blood flow: In vivo imaging veritas. Trends in Neuroscience. 2019;42:528–536
30. Denk W, Strickler JH, Webb WW. Two-photon laser scanning fluorescence microscopy. Science. 1990;248:73–76 [PubMed: 2321027]
31. Holtmaat A, Svoboda K. Experience-dependent structural synaptic plasticity in the mammalian brain. Nature Reviews Neuroscience. 2009;10:647–658 [PubMed: 19693029]

32. Tian L, Hires SA, Mao T, Huber D, Chiappe ME, Chalasani SH, Petreanu L, Akerboom J, McKinney SA, Schreiter ER, et al. Imaging neural activity in worms, flies and mice with improved GCaMP calcium indicators. Nature Methods. 2009;6:875–881 [PubMed: 19898485]
33. Petzold GC, Murthy VN. Role of astrocytes in neurovascular coupling. Neuron. 2011;71:782–797 [PubMed: 21903073]
34. Dirnagl U, Villringer A, Einhaupl KM. *In-vivo* confocal scanning laser microscopy of the cerebral microcirculation. Journal of Microscopy. 1992;165:147–157 [PubMed: 1552568]
35. Kleinfeld D, Mitra PP, Helmchen F, Denk W. Fluctuations and stimulus-induced changes in blood flow observed in individual capillaries in layers 2 through 4 of rat neocortex. Proceedings of the National Academy of Sciences USA. 1998;95:15741–15746
36. Hartmann DA, Underly RG, Watson AN, Shih AY. A murine toolbox for imaging the neurovascular unit. Microcirculation. 2015;22:168–182 [PubMed: 25352367]
37. Masamoto K, Vazquez A. Optical imaging and modulation of neurovascular responses. Journal of cerebral blood flow and metabolism. 2018;38:2057–2072 [PubMed: 30334644]
38. Rungta RL, Chaigneau E, Osmanski BF, Charpak S. Vascular compartmentalization of functional hyperemia from the synapse to the pia. Neuron. 2018;99:362–375 [PubMed: 29937277]
39. Mishra A, Reynolds JP, Chen Y, Gourine AV, Rusakov DA, Attwell D. Astrocytes mediate neurovascular signaling to capillary pericytes but not to arterioles. Nature Neuroscience. 2016;19:1619–1627 [PubMed: 27775719]
40. Tran CHT, Peringod G, Gordon GR. Astrocytes integrate behavioral state and vascular signals during functional hyperemia. Neuron. 2018;100:1133–1148 [PubMed: 30482689]
41. Hill RA, Tong L, Yuan P, Murikinati S, Gupta S, Grutzendler J. Regional blood flow in the normal and ischemic brain is controlled by arteriolar smooth muscle cell contractility and not by capillary pericytes. Neuron. 2015;87:95–110 [PubMed: 26119027]
42. Longden TA, Dabertrand F, Koide M, Gonzales AL, Tykocki NR, Brayden JE, Hill-Eubanks D, Nelson MT. Capillary K+-sensing initiates retrograde hyperpolarization to increase local cerebral blood flow. Nature Neuroscience. 2017;20:717–726 [PubMed: 28319610]
43. O'Herron P, Chhatbar PR, Levy M, Shen Z, Schramm AE, Lu Z, Kara P. Neural correlates of single-vessel haemodynamic responses in vivo. Nature. 2016;534:378–382 [PubMed: 27281215]
44. Harb R, Whiteus C, Freitas C, Grutzendler J. In vivo imaging of cerebral microvascular plasticity from birth to death. Journal of Cerebral Blood Flow & Metabolism. 2012;33:146–156 [PubMed: 23093067]
45. Coelho-Santos V, Berthiaume AA, Ornelas S, Stuhlmann H, Shih AY. Imaging the construction of capillary networks in the neonatal mouse brain. Proc Natl Acad Sci U S A. 2021;118:e2100866118 [PubMed: 34172585]
46. Letourneur A, Chen V, Waterman G, Drew PJ. A method for longitudinal, transcranial imaging of blood flow and remodeling of the cerebral vasculature in postnatal mice. Physiological Reports. 2014;2:e12238 [PubMed: 25524276]
47. Borjini N, Paouri E, Tognatta R, Akassoglou K, Davalos D. Imaging the dynamic interactions between immune cells and the neurovascular interface in the spinal cord. Experimental Neurology. 2019;322:113046 [PubMed: 31472115]
48. Cruz Hernández JC, Bracko O, Kersbergen CJ, Muse V, Haft-Javaherian M, Berg M, Park L, Vinarcsik LK, Ivasyk I, Rivera DA, et al. Neutrophil adhesion in brain capillaries reduces cortical blood flow and impairs memory function in Alzheimer's disease mouse models. Nature Neuroscience. 2019;22:413–420 [PubMed: 30742116]
49. Devor A, Sakadzic S, Saisan PA, Yaseen MA, Roussakis E, Srinivasan VJ, Vinogradov SA, Rosen BR, Buxton RB, Dale AM, et al. "Overshoot" of O_2 is required to maintain baseline tissue oxygenation at locations distal to blood vessels. Journal of Neuroscience. 2011;31:13676–13681 [PubMed: 21940458]
50. Kisler K, Nelson AR, Rege SV, Ramanathan A, Wang Y, Ahuja A, Lazic D, Tsai PS, Zhao Z, Zhou Y, et al. Pericyte degeneration leads to neurovascular uncoupling and limits oxygen supply to brain. Nature Neuroscience. 2017;20:406–416 [PubMed: 28135240]

51. Li B, Esipova TV, Sencan I, Kılıç K, Fu B, Desjardins M, Moeini M, Kura S, Yaseen MA, Lesage F, et al. More homogeneous capillary flow and oxygenation in deeper cortical layers correlate with increased oxygen extraction. Elife. 2019;8: e42299 [PubMed: 31305237]
52. Esipova TV, Barrett MJP, Erlebach E, Masunov AE, Weber B, Vinogradov SA. Oxyphor 2p: A high-performance probe for deep-tissue longitudinal oxygen imaging. Cell Metabolism. 2019;S1550–4131:30759–30759
53. Kucharz K, Kristensen K, Johnsen KB, Lund MA, M. L, Moos T, Andresen TL, Lauritzen MJ. Post-capillary venules are the key locus for transcytosis-mediated brain delivery of therapeutic nanoparticles. Nature Communications. 2021;12:4121
54. Bell RD, Winkler EA, Singh I, Sagare AP, Deane R, Wu Z, Holtzman DM, Betsholtz C, Armulik A, Sallstrom J, et al. Apolipoprotein e controls cerebrovascular integrity via cyclophilin a. Nature. 2012;485:512–516 [PubMed: 22622580]
55. van Veluw SJ, Hou SS, Calvo-Rodriguez M, Arbel-Ornath M, Snyder AC, Frosch MP, Greenberg SM, Bacskai BJ. Vasomotion as a driving force for paravascular clearance in the awake mouse brain. Neuron. 2020;105:549–561 [PubMed: 31810839]
56. Iliff JJ, Wang M, Liao Y, Plogg BA, Peng W, Gundersen GA, Benveniste H, Vates GE, Deane R, Goldman SA, et al. A paravascular pathway facilitates csf flow through the brain parenchyma and the clearance of interstitial solutes, including amyloid β. Science Translational Medicine. 2012;4:147ra111
57. Kobat D, Durst ME, Nishimura N, Wong AW, Schaffer CB, Xu C. Deep tissue multiphoton microscopy using longer wavelength excitation. Optics Express. 2009;17:13354–13364 [PubMed: 19654740]
58. Miller DR, Hassan AM, Jarrett JW, Medina FA, Perillo EP, Hagan K, Shams Kazmi SM, Clark TA, Sullender CT, Jones TA, et al. In vivo multiphoton imaging of a diverse array of fluorophores to investigate deep neurovascular structure. Biomedical Optics Express. 2017;8:3470–3481 [PubMed: 28717582]
59. Kobat D, Horton NG, Xu C. In vivo two-photon microscopy to 1.6-mm depth in mouse cortex. Journal of Biomedical Optics. 2011;16:106014 [PubMed: 22029361]
60. Li B, Ohtomo R, Thunemann M, Adams SR, Yang J, Fu B, Yaseen MA, Ran C, Polimeni JR, Boas DA, et al. Two-photon microscopic imaging of capillary red blood cell flux in mouse brain reveals vulnerability of cerebral white matter to hypoperfusion. Journal of Cerebral Blood Flow & Metabolism. 2019;40:501–512 [PubMed: 30829101]
61. Helmchen F, Denk W. Deep tissue two-photon microscopy. Nature Methods. 2005;2:932–940 [PubMed: 16299478]
62. Theer P, Denk W. On the fundamental imaging-depth limit in two-photon microscopy. Journal of the Americal Optical Society A. 2006;23:3139–3150
63. Horton NG, Wang K, Kobat D, Clark CG, Wise FW, Schaffer CB, Xu C. In vivo three-photon microscopy of subcortical structures within an intact mouse brain. Nature Photonics. 2013;7:10.1038/nphoton.2012.1336.
64. Takasaki K, Abbasi-Asl R, Waters J. Superficial bound of the depth limit of 2-photon imaging in mouse brain. eNeuro. 2020;7:ENEURO.0255–0219.2019
65. Liu CJ, Roy A, Simons AA, Farinella DM, Kara P. Three-photon imaging of synthetic dyes in deep layers of the neocortex. Scientific Reports. 2020;10:16351 [PubMed: 33004996]
66. Hontani Y, Xia F, Xu C. Multicolor three-photon fluorescence imaging with single-wavelength excitation deep in mouse brain. Science Advances. 2021;7:eabf3531 [PubMed: 33731355]
67. Thornton MA, Futia GL, Stockton ME, Ozbay BN, Kilborn K, Restrepo D, Gibson EA, Hughes EG. Characterization of red fluorescent reporters for dual-color in vivo three-photon microscopy. Neurophotonics. 2022;9:031912 [PubMed: 35496497]
68. Ouzounov DG, Wang T, Wang M, Feng DD, Horton NG, Cruz-Hernández JC, Cheng YT, Reimer J, Tolias AS, Nishimura N, et al. In vivo three-photon imaging of activity of GCaMP6-labeled neurons deep in intact mouse brain. Nature Methods. 2017;14:388–390 [PubMed: 28218900]
69. Yildirim M, Sugihara H, So PTC, Sur M. Functional imaging of visual cortical layers and subplate in awake mice with optimized three-photon microscopy. Nature Communications. 2019;10:177

70. Liu H, Wang J, Zhuang Z, He J, Wen W, Qiu P, Wang K. Visualizing astrocytes in the deep mouse brain in vivo. Journal of Biophotonics. 2019;12:e201800420 [PubMed: 30938095]
71. Montagne A, Nation DA, Sagare AP, Barisano G, Sweeney MD, Chakhoyan A, Pachicano M, Joe E, Nelson AR, D'Orazio LM, et al. Apoe4 leads to blood-brain barrier dysfunction predicting cognitive decline. Nature. 2020;581:71–76 [PubMed: 32376954]
72. Huang D, Swanson EA, Lin CP, Schuman JS, Stinson WG, Chang W, Hee MR, Flotte T, Gregory K, Puliafito CAea. Optical coherence tomography. Science. 1991;254:1178–1181 [PubMed: 1957169]
73. Fujimoto JG, Pitris C, Boppart SA, Brezinski ME. Optical coherence tomography: An emerging technology for biomedical imaging and optical biopsy. Neoplasia. 2000;2:9–25 [PubMed: 10933065]
74. Mariampillai A, Leung MK, Jarvi M, Standish BA, Lee K, Wilson BC, Vitkin A, Yang VXOLA-dOP. Optimized speckle variance oct imaging of microvasculature. Optics Letters. 2010;35:1257–1259 [PubMed: 20410985]
75. Jia Y, Tan O, Tokayer J, Potsaid B, Wang Y, Liu JJ, Kraus MF, Subhash H, Fujimoto JG, Hornegger J, et al. Split-spectrum amplitude-decorrelation angiography with optical coherence tomography. Optics Express. 2012;20:4710–4725 [PubMed: 22418228]
76. Li Y, Tang P, Song S, Rakymzhan A, Wang RK. Electrically tunable lens integrated with optical coherence tomography angiography for cerebral blood flow imaging in deep cortical layers in mice. Optics Letters. 2019;44:5037–5040 [PubMed: 31613257]
77. Duvernoy HM, Delon S, L. VJ. Cortical blood vessels of the human brain. Brain Research Bulletin. 1981;7:519–579 [PubMed: 7317796]
78. Park KS, Shin JG, Qureshi MM, Chung E, Eom TJ. Deep brain optical coherence tomography angiography in mice: In vivo, noninvasive imaging of hippocampal formation. Scientific Reports. 2018;8:11614 [PubMed: 30072791]
79. Shi L, Qin J, Reif R, Wang RK. Wide velocity range doppler optical microangiography using optimized step-scanning protocol with phase variance mask. Journal of Biomedical Optics. 2013;18:106015 [PubMed: 24165741]
80. Li Y, Rakymzhan A, Tang P, Wang RK. Procedure and protocols for optical imaging of cerebral blood flow and hemodynamics in awake mice. Biomedical Optics Express. 2020;11:3288–3300 [PubMed: 32637255]
81. Chen Z, Milner TE, Srinivas S, Wang X, Malekafzali A, van Gemert MJ, Nelson JS. Noninvasive imaging of in vivo blood flow velocity using optical doppler tomography. Optics Letters. 1997;22:119–1121
82. Baran U, Li Y, Wang RK. Vasodynamics of pial and penetrating arterioles in relation to arteriolo-arteriolar anastomosis after focal stroke. Neurophotonics. 2015;2:025006 [PubMed: 26158010]
83. Kanoke A, Akamatsu Y, Nishijima Y, To E, Lee CC, Li Y, Wang RK, Tominaga T, Liu J. The impact of native leptomeningeal collateralization on rapid blood flow recruitment following ischemic stroke. Journal of cerebral blood flow and metabolism. 2020;40:2165–2178 [PubMed: 32669022]
84. Srinivasan VJ, Mandeville ET, Can A, Blasi F, Climov M, Daneshmand A, Lee JH, Yu E, Radhakrishnan H, Lo EH, et al. Multiparametric, longitudinal optical coherence tomography reveals acute injury and chronic recovery in experimental ischemic stroke. PLoS One. 2013;8:871478v
85. Li Y, Choi WJ, Wei W, Song S, Zhang Q, Liu J, Wang RK. Aging-associated changes in cerebral vasculature and blood flow as determined by quantitative optical coherence tomography angiography. Neurobiology of Aging. 2018;70:148–159 [PubMed: 30007164]
86. Srinivasan VJ, Radhakrishnan H, Lo EH, Mandeville ET, Jiang JY, Barry S, Cable AE. OCT methods for capillary velocimetry. Biomedical Optics Express. 2012;3:612–629 [PubMed: 22435106]
87. Lee J, Wu W, Lesage F, Boas DA. Multiple-capillary measurement of RBC speed, flux, and density with optical coherence tomography. Journal of Cerebral Blood Flow & Metabolism. 2013;33:1707–1710 [PubMed: 24022621]

88. Wang RK, Zhang Q, Li Y, Song S. Optical coherence tomography angiography-based capillary velocimetry. Journal of Biomedical Optics. 2017;22:66008 [PubMed: 28617921]
89. Li Y, Wei W, Wang RK. Capillary flow homogenization during functional activation revealed by optical coherence tomography angiography based capillary velocimetry. Scientific Reports. 2018;8:4107 [PubMed: 29515156]
90. Jespersen SN, Østergaard L. The roles of cerebral blood flow, capillary transit time heterogeneity, and oxygen tension in brain oxygenation and metabolism. Journal of Cerebral Blood Flow & Metabolism. 2012;32:264–277 [PubMed: 22044867]
91. Østergaard L, Jespersen SN, Engedahl T, Gutiérrez J,E, Ashkanian M, Hansen MB, Eskildsen S, Mouridsen K. Capillary dysfunction: Its detection and causative role in dementias and stroke. Current neurology and neuroscience reports. 2015;15:37 [PubMed: 25956993]
92. Srinivasan VJ, Radhakrishnan H, Jiang JY, Barry S, Cable AE. Optical coherence microscopy for deep tissue imaging of the cerebral cortex with intrinsic contrast. Optics Express. 2012;20:2220–2239 [PubMed: 22330462]
93. Zhu J, Freitas HR, Maezawa I, Jin LW, Srinivasan VJ. 1700 nm optical coherence microscopy enables minimally invasive, label-free, in vivo optical biopsy deep in the mouse brain. Light, Science and Applications 2021;10:145
94. Xia J, Yao J, Wang LV. Photoacoustic tomography: Principles and advances. Electromagnetic waves. 2014;147:1–22 [PubMed: 25642127]
95. Wang X, Pang Y, Ku G, Xie X, Stoica G, Wang LV. Noninvasive laser-induced photoacoustic tomography for structural and functional in vivo imaging of the brain. Nature Biotechnology. 2003;21:803–806
96. Laufer J, Zhang E, Raivich G, Beard P. Three-dimensional noninvasive imaging of the vasculature in the mouse brain using a high resolution photoacoustic scanner. Applied Optics. 2009;48:D299–306 [PubMed: 19340121]
97. Zhang P, Li L, Lin L, Hu P, Shi J, He Y, Zhu L, Zhou Y, Wang LV. High-resolution deep functional imaging of the whole mouse brain by photoacoustic computed tomography in vivo. Journal of Biophotonics. 2018;11
98. Ning B, Sun N, Cao R, Chen R, Kirk Shung K, Hossack JA, Lee JM, Zhou Q, Hu S. Ultrasound-aided multi-parametric photoacoustic microscopy of the mouse brain. Scientific Reports. 2015;5:18775 [PubMed: 26688368]
99. Zhu X, Huang Q, DiSpirito A, Vu T, Rong Q, Peng X, Sheng H, Shen X, Zhou Q, Jiang L, et al. Real-time whole-brain imaging of hemodynamics and oxygenation at micro-vessel resolution with ultrafast wide-field photoacoustic microscopy. Light: Science and Applications. 2022;11
100. Cao R, Li J, Ning B, Sun N, Wang T, Zuo Z, Hu S. Functional and oxygen-metabolic photoacoustic microscopy of the awake mouse brain. Neuroimaging. 2017;150:77–87
101. Ni R, Rudin M, Klohs J. Cortical hypoperfusion and reduced cerebral metabolic rate of oxygen in the ArcAβ mouse model of Alzheimer's disease. Photoacoustics. 2018;10:38–47 [PubMed: 29682448]
102. Maslov K, Zhang HF, Hu S, Wang LV. Optical-resolution photoacoustic microscopy for in vivo imaging of single capillaries. Optics Letters. 2008;33:929–931 [PubMed: 18451942]
103. Hu S, Yan P, Maslov K, Lee JM, Wang LVOLD-dOPPP. Intravital imaging of amyloid plaques in a transgenic mouse model using optical-resolution photoacoustic microscopy. Optics Letters. 2009;34:3899–3901 [PubMed: 20016651]
104. Macé E, Montaldo G, Cohen I, Baulac M, Fink M, Tanter M. Functional ultrasound imaging of the brain. Nature Methods. 2011;8:662–664 [PubMed: 21725300]
105. Brunner C, Grillet M, Urban A, Roska B, Montaldo G, Macé E. Whole-brain functional ultrasound imaging in awake head-fixed mice. Nature Protocols. 2021;16:3547–3571 [PubMed: 34089019]
106. Tournissac M, Boido D, Omnès M, Houssen YG, Ciobanu L, Charpak S. Cranial window for longitudinal and multimodal imaging of the whole mouse cortex. Neurophotonics. 2022;9:031921 [PubMed: 36159711]

107. Macé É, Montaldo G, Trenholm S, Cowan C, Brignall A, Urban A, Roska B. Whole-brain functional ultrasound imaging reveals brain modules for visuomotor integration. Neuron. 2018;100:1241–1251 [PubMed: 30521779]
108. Errico C, Pierre J, Pezet S, Desailly Y, Lenkei Z, Couture O, Tanter M. Ultrafast ultrasound localization microscopy for deep super-resolution vascular imaging. Nature. 2015;527:499–502 [PubMed: 26607546]
109. Lowerison MR, Sekaran NVC, Zhang W, Dong Z, Chen X, Llano DA, Song P. Aging-related cerebral microvascular changes visualized using ultrasound localization microscopy in the living mouse. Scientific Reports. 2022;12:619 [PubMed: 35022482]
110. Keith J, Gao FQ, Noor R, Kiss A, Balasubramaniam G, Au K, Rogaeva E, Masellis M, Black SE. Collagenosis of the deep medullary veins: An under-recognized pathologic correlate of white matter hyperintensities and periventricular infarction? Journal of neuropathology and experimental neurology. 2017;76:299–312 [PubMed: 28431180]
111. Lai AY, Dorr A, Thomason LA, Koletar MM, Sled JG, Stefanovic B, McLaurin J. Venular degeneration leads to vascular dysfunction in a transgenic model of alzheimer's disease. Brain. 2015;138:1046–1058 [PubMed: 25688079]
112. Brown WR, Thore CR. Cerebral microvascular pathology in aging and neurodegeneration. Neuropathology and applied neurobiology. 2011;37:56–74 [PubMed: 20946471]
113. Ali M, Falkenhain K, Njiru BN, Murtaza-Ali M, Ruiz-Uribe NE, Haft-Javaherian M, Catchers S, Nishimura N, Schaffer CB, Bracko O. VEGF signalling causes stalls in brain capillaries and reduces cerebral blood flow in alzheimer's mice. Brain. 2022;145:1449–1463 [PubMed: 35048960]
114. Eskildsen SF, Gyldensted L, Nagenthiraja K, Nielsen RB, Hansen MB, Dalby RB, Frandsen J, Rodell A, Gyldensted C, Jespersen SN, et al. Increased cortical capillary transit time heterogeneity in Alzheimer's disease: A DSC-MRI perfusion study. 50. 2017:107–118
115. Damisah EC, Hill RA, Tong L, Murray KN, Grutzendler J. A fluoro-nissl dye identifies pericytes as distinct vascular mural cells during in vivo brain imaging. Nature Neuroscience. 2017;20:1023–1032 [PubMed: 28504673]
116. Gutiérrez-Jiménez E, Angleys H, Rasmussen PM, West MJ, Catalini L, Iversen NK, Jensen MS, Frische S, Østergaard L. Disturbances in the control of capillary flow in an aged APPswe/PS1δe9 model of alzheimer's disease. Neurobiology of Aging. 2018;62:82–94 [PubMed: 29131981]
117. Gerhardt H, Betsholtz C. Endothelial-pericyte interactions in angiogenesis. Cell and Tissue Research. 2003;314:15–23 [PubMed: 12883993]
118. Armulik A, Genové G, Mäe M, Nisancioglu MH, Wallgard E, Niaudet C, He L, Norlin J, Lindblom P, Strittmatter K, et al. Pericytes regulate the blood-brain barrier. Nature. 2010;468:557–561 [PubMed: 20944627]
119. Daneman R, Zhou L, Kebede AA, Barres BA. Pericytes are required for blood-brain barrier integrity during embryogenesis. Nature. 2010;468:562–566 [PubMed: 20944625]
120. Bell RD, Winkler EA, Sagare AP, Singh I, LaRue B, Deane R, Zlokovic BV. Pericytes control key neurovascular functions and neuronal phenotype in the adult brain and during brain aging. Neuron. 2010;68:409–427 [PubMed: 21040844]
121. Soto I, Graham LC, Richter HJ, Simeone SN, Radell JE, Grabowska W, Funkhouser WK, Howell MC, Howell GR. Apoe stabilization by exercise prevents aging neurovascular dysfunction and complement induction. Plos Biology. 2015;13:e1002279 [PubMed: 26512759]
122. Sengillo JD, Winkler EA, Walker CT, Sullivan JS, Johnson M, Zlokovic BV. Deficiency in mural vascular cells coincides with blood-brain barrier disruption in Alzheimer's disease. Brain Pathology. 2013;23:303–310 [PubMed: 23126372]
123. Halliday MR, Rege SV, Ma Q, Zhao Z, Miller CA, Winkler EA, Zlokovic BV. Accelerated pericyte degeneration and blood-brain barrier breakdown in apolipoprotein e4 carriers with Alzheimer's disease. Journal of Cerebral Blood Flow & Metabolism. 2016;36:216–227 [PubMed: 25757756]
124. Schultz N, Brännström K, Byman E, Moussaud S, Nielsen HM, Bank NB, Olofsson A, Wennström M. Amyloid-beta 1–40 is associated with alterations in ng2+ pericyte population ex vivo and in vitro. Aging Cell. 2018;17:e12728 [PubMed: 29453790]

125. Ding R, Hase Y, Ameen-Ali KE, Ndung'u M, Stevenson W, Barsby J, Gourlay R, Akinyemi T, Akinyemi R, Uemura MT, et al. Loss of capillary pericytes and the blood-brain barrier in white matter in poststroke and vascular dementias and Alzheimer's disease. Brain Pathology. 2020;30:1087–1101 [PubMed: 32705757]

126. Choe YG, Yoon JH, Joo J, Kim B, Hong SP, Koh GY, Lee DS, Oh DY, Jeong Y. Pericyte loss leads to capillary stalling through increased leukocyte-endothelial cell interaction in the brain. Frontiers in Cellular Neuroscience. 2022;16:848764 [PubMed: 35360491]

127. Berthiaume AA, Schmid F, Stamenkovic S, Coelho-Santos V, Nielson CD, Weber B, Majesky MW, Shih AY. Pericyte remodeling is deficient in the aged brain and contributes to impaired capillary flow and structure. Nature Communications. 2022; 13(1):5912.

128. Nortley R, Korte N, Izquierdo P, Hirunpattarasilp C, Mishra A, Jaunmuktane Z, Kyrargyri V, Pfeiffer T, Khennouf L, Madry C, et al. Amyloid β oligomers constrict human capillaries in Alzheimer's disease via signaling to pericytes. Science. 2019;365:Epub 2019 Jun 2020

129. Rajpoot J, Crooks EJ, Irizarry BA, Amundson A, Van Nostrand WE, Smith SO. Insights into cerebral amyloid angiopathy type 1 and type 2 from comparisons of the fibrillar assembly and stability of the Aβ40-iowa andAβ40-dutch peptides. Biochemistry. 2022;61:1181–1198 [PubMed: 35666749]

130. Shaw K, Bell L, Boyd K, Grijseels DM, Clarke D, Bonnar O, Crombag HS, Hall CN. Neurovascular coupling and oxygenation are decreased in hippocampus compared to neocortex because of microvascular differences. Nature Communications. 2021;12:3190

131. Rivera AD, Pieropan F, Chacon-De-La-Rocha I, Lecca D, Abbracchio MP, Azim K, Butt AM. Functional genomic analyses highlight a shift in gpr17-regulated cellular processes in oligodendrocyte progenitor cells and underlying myelin dysregulation in the aged mouse cerebrum. Aging cell. 2021;20:e13335 [PubMed: 33675110]

132. Peters A, Sethares C. Aging and the myelinated fibers in prefrontal cortex and corpus callosum of the monkey. Journal of Comparitive Neurology. 2002;442:277–291

133. Meier-Ruge W, Ulrich J, Brühlmann M, Meier E. Age-related white matter atrophy in the human brain. Annals of the New York Academy of Sciences. 1992;673:260–269 [PubMed: 1485724]

134. Peters A The effects of normal aging on myelinated nerve fibers in monkey central nervous system. Frontiers in Neuroanatomy. 2009;3:11 [PubMed: 19636385]

135. Papuć E, Rejdak K. The role of myelin damage in Alzheimer's disease pathology. Archives of Medical Science. 2018;16:345–351 [PubMed: 32190145]

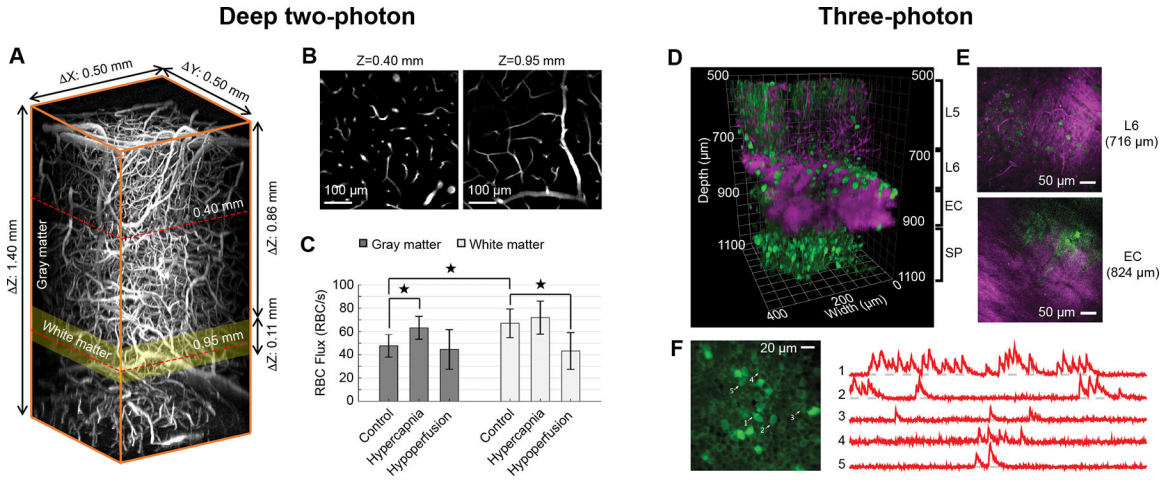

Figure 1. In vivo imaging with deep 2PM and 3PM.

(A) Volume of tissue showing microvasculature in cortex, callosal white matter, and hippocampus, captured by deep 2P in vivo using Alexa 680-dextran dye. **(B)** Planar view at two imaging depths (Z = 0.40 mm and 0.95 mm below the brain surface) outlined by the red dashed lines in panel A. **(C)** Bar plots of average capillary RBC flux in the cerebral gray and white matter, during control conditions, mild hypercapnia and global cerebral hypoperfusion, respectively. Data are expressed as mean ± SD. *P < 0.05, Student's t-test. Li et al., Journal of Cerebral Blood Flow and Metabolism (volume 40, issue 3), pp. 501–512, copyright ©2019 by (Sage Publications), reprinted by Permission of SAGE Publication.[60] **(D)** Volume collected by 3PM showing GCaMP6s-labeled neurons in the mouse cortex and the hippocampus (green, GCaMP6 fluorescence; magenta, intrinsic third-harmonic signal (THG)). **(E)** Planar views showing cortical layer 6 (L6) and external capsule (EC) from panel D. THG visualizes blood vessels and myelinated axons in the EC. **(F)** Neuronal activity recording site in the hippocampus located at 984 µm. Traces on the right show spontaneous activity recorded from the labeled neurons indicated in panel F. Adapted from Ouzounov et al.[68] with permission. Copyright ©2017, Springer Nature.

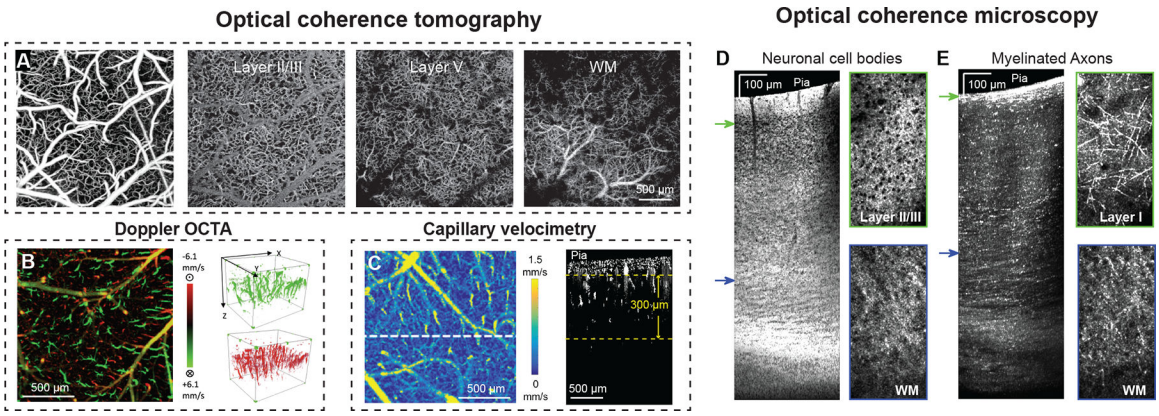

Figure 2. In vivo imaging with OCTA and OCM.

(A) Volume of OCTA data collected in mouse cortex through a cranial window. Planar view maximum intensity projections (MIP) at different depths. WM: White matter. **(B)** Bi-directional axial velocity map generated by en face MIP of the 3D doppler OCTA data. Color bar represents the RBC axial velocity of the flow descending into (positive, green) and rising from (negative, red) the cortical surface. The 3D velocity signals are shown to the right of the projection image. **(C)** En face average intensity projection of the 3D capillary velocimetry dataset within a 300 µm thick region of cortex. Color represents a blood flow velocity range. A cross section at the white-dashed line position is shown to the right. Reprinted with permission from 76 © The Optical Society. Reprinted with permission from 80 © The Optical Society Used with permission of SPIE, from Optical coherence tomography angiography-based capillary velocimetry, Wang RK, 22, 2017; permission conveyed through Copyright Clearance Center, Inc.[88] **(D)** OCM imaging of neuronal cell bodies with side view of tissue on the left and en face projection view on the right. Outline colors of the en face images correspond to z depth as indicated by the arrow colors on the side view. **(E)** Myelinated axons shown with side view of tissue on the left and en face projection at two selected z depths. Side view slice projection thickness: 190 µm. Axial projection thickness: 11.2 µm. Adapted from Zhu et al.[93]

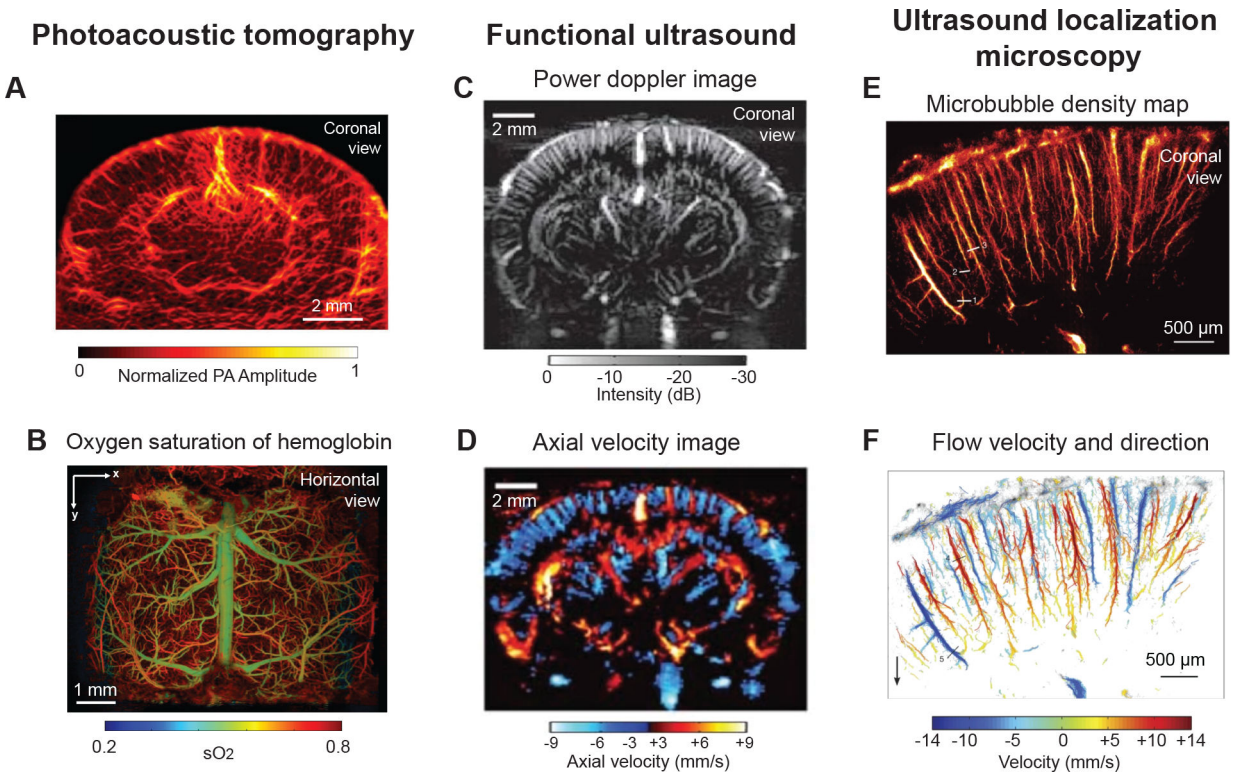

Figure 3. In vivo imaging with ultrasound-based technologies.

(A) Photoacoustic computed tomography image providing coronal view of mouse brain through an intact skull. Used with permission of John Wiley & Sons, from High-resolution deep functional imaging of the whole mouse brain by photoacoustic computed tomography in vivo, Zhang P, 11, 2018; permission conveyed through Copyright Clearance Center, Inc.[97] **(B)** Horizontal view showing oxygen saturation of blood in vasculature from dorsal surface of mouse brain, collected by ultra-fast wide-field photoacoustic microscopy. Images were collected after skull removal and implantation of a whole cortex window. Adapted from Zhu et al.[99] **(C,D)** Entire depth of rat brain imaged through a bihemispheric transcranial window using fUS. Panel C shows power Doppler image and panel D shows axial blood velocity image revealing domains perfused by penetrating vessels. Adapted from Macé et al.[104] with permission. Copyright ©2011, Springer Nature. **(E,F)** Magnified view of cortical microvessels imaged by ultrasound localization microscopy. Panel E shows microbubble density map and panel F shows flow velocity and flow direction map revealing individual cortical penetrating arterioles and ascending venules. Adapted from Errico et al.[108] with permission. Copyright ©2015, Springer Nature.

Table 1.

Applications and characteristics of deep optical imaging modalities

	Mechanism of signal generation	Measurable features	Spatial resolution	Practical imaging depth
Two-photon microscopy	Fluorescence	Cell morphology and activity, vascular structure, and blood flow	~1–5 μm	~0.5 mm
Deep Two-photon microscopy	Fluorescence	Cell morphology, vascular structure, and blood flow	~1–5 μm	~1.2 mm
Three-photon microscopy	Fluorescence	Cell morphology and activity, vascular structure, and blood flow	~1–5 μm	~1.2 mm
Optical coherence tomography angiography	Optical scattering	Vascular structure and blood flow	~10–15 μm	~2 mm
Optical coherence microscopy	Optical scattering	Neuron structure and myelination	~3 μm	~2 mm
Photoacoustic imaging	Optical energy absorption and sound wave detection	Vascular structure, blood flow and blood oxygen content	~10–100 μm	~1–3 mm
Functional ultrasound imaging	Sound energy absorption and wave detection	Vascular structure and blood flow	~100 μm (~10 μm with Ultrasound Localization Microscopy	~1 cm

Table 2.

Advantages and disadvantages of deep optical imaging modalities

Imaging modality	Advantages	Disadvantages
Deep two-photon microscopy	High-resolution in vivo imaging of vascular structure, function, and cell types.	Deep 2PM is effective for only red/far red dyes and proteins. Typically requires introduction of exogenous fluorophores.
Three-photon microscopy	High-resolution in vivo imaging of vascular structure, function and cell types. Visualization of the cortical gray/white matter boundary through intrinsic third harmonic signal generation. Multi-color imaging for concurrent investigation of neuronal activity and vascular function.	Requires cranial windows, which can disrupt the intracranial environment Slower image acquisition is better suited for single vessel studies. Imaging is limited in field of view. Possibility of photodamage due to high laser powers.
Optical coherence tomography angiography	High-resolution in vivo imaging of microvascular structure and blood flow without exogenous contrast agents. High throughput capillary velocity and flux measurement in the microvascular network	Unable to image neurovascular cell types. Typically examined as x–y projections and tracing vessel structures in 3D is problematic. Limited penetration depth for capillary velocimetry (up to 500 μm). Strong scattering caused by larger vessels at the brain surface leads to imaging artifacts at depth. Requires cranial windows.
Optical coherence microscopy	High throughput mapping of neuronal and myelinated structures.	Limited ability to visualize neurovascular cell types.
Photoacoustic imaging	Imaging of vascular structure and blood oxygen across networks with single arteriole and venular resolution. Some adaptations allow visualization of vasculature in whole brain cross sections in vivo. Imaging can be performed through an intact skull for some applications	Unable to image neurovascular cell types. Possibility of photodamage due to high laser power. Shadowing of the larger vessels at brain surface leads to imaging artifacts
Functional ultrasound imaging	Imaging of vascular structure and function through the entire rodent brain. Imaging performed through an intact skull. Skull-thinning required for high resolution. Device is portable	Unable to image neurovascular cell types. Does not allow for investigation at the level of capillary networks.